Electronic Supporting Information for :

Nitro and nitritosilanes: Do they and can they exist?

H. Dahmani, L.-P. Poulin, C.-É. Fecteau, L. Harter, P. A. Johnson and G. Bélanger-Chabot*.

Experimental Details

Silver nitrite was synthesized and isolated by precipitation from $AgNO_3$ and $NaNO_2$ aqueous solutions and was dried under vacuum overnight. The silyl chlorides were purchased from Sigma-Aldrich and used without purification. All manipulations were conducted under inert atmosphere using high vacuum line, Schlenk and glovebox techniques. Deuterated solvents were dried over 3 Å molecular sieves and degassed by freeze-pump-thaw cycles before use. Other solvents were distilled and degassed, then stored under nitrogen over activated 3 Å molecular sieves. Liquid-phase NMR spectra were recorded on a 500 MHz NMR spectrometer (^{1}H: 500 MHz, ^{13}C: 125 MHz, ^{29}Si: 99 MHz, ^{14}N: 36 MHz). Chemical shifts (δ) are reported in ppm and referenced internally to the solvent signal (^{13}C NMR), to the residual protic signal (^{1}H NMR) of the deuterated solvent, or to the protic signal of protic solvent (^{1}H NMR). ^{29}Si and ^{14}N chemical shifts were externally referenced to tetramethylsilane and nitromethane, respectively. IR spectra of isolated compounds were obtained neat in the nitrogen atmosphere of a glovebox using a Bruker Alpha spectrometer equipped with a diamond-ATR module. Gas-phase IR spectra were acquired in a glass cell equipped with a Teflon valve and NaCl windows, with a 5 cm optical path. Raman spectra were recorded using a Bruker Multiram FT spectrometer in sealed J.Y.-style NMR tubes.

Synthesis and isolation of *tert*-butyldimethylnitritosilane (1)

The reaction was performed in a vial inside a glovebox. *Tert*-butyldimethylsilyl chloride (*t*$BuMe_2SiCl$) (136 mg, 0.905 mmol) was added to silver nitrite ($AgNO_2$) (139 mg, 0.905) mmol) suspended in 3 mL pentane. Following the addition, a precipitate of AgCl formed after a few minutes. The reaction mixture was stirred for approximately 12 h, and the reaction was monitored using ^{1}H and ^{14}N NMR spectroscopy, confirming 100% conversion. The precipitate was decanted off and the supernatant was placed in glass reactor. The solvent was removed *in vacuo* from the solution, which was maintained at *ca.* -63°C to prevent the volatile product from escaping. After 3 h under vacuum, the product was successfully isolated in 29 % yield as a pale yellow to colorless liquid. The compound is solid at -30°C. It remains stable in solution without significant decomposition for several days.

<u>^{1}H NMR</u> (CD_3CN): δ=0.40 ppm (s, 6H, $Si(CH_3)_2tBu$), δ=0.96 ppm (s, 9H, $SiMe_2C(CH_3)_3$)

^{14}N NMR (CD_3CN): δ=197 ppm (s, ONO)

^{13}C{^{1}H}top NMR (CD_3CN): δ=-4.6 ppm (s, 2C, *C*H_3-Si), δ=18.8 ppm (s, 3C, (*C*H_3)$_3$-C), δ=25.8 ppm (s, 1C, *C*Me_3)

^{29}Si NMR (CD_3CN): δ=32.1 ppm (s, Si)

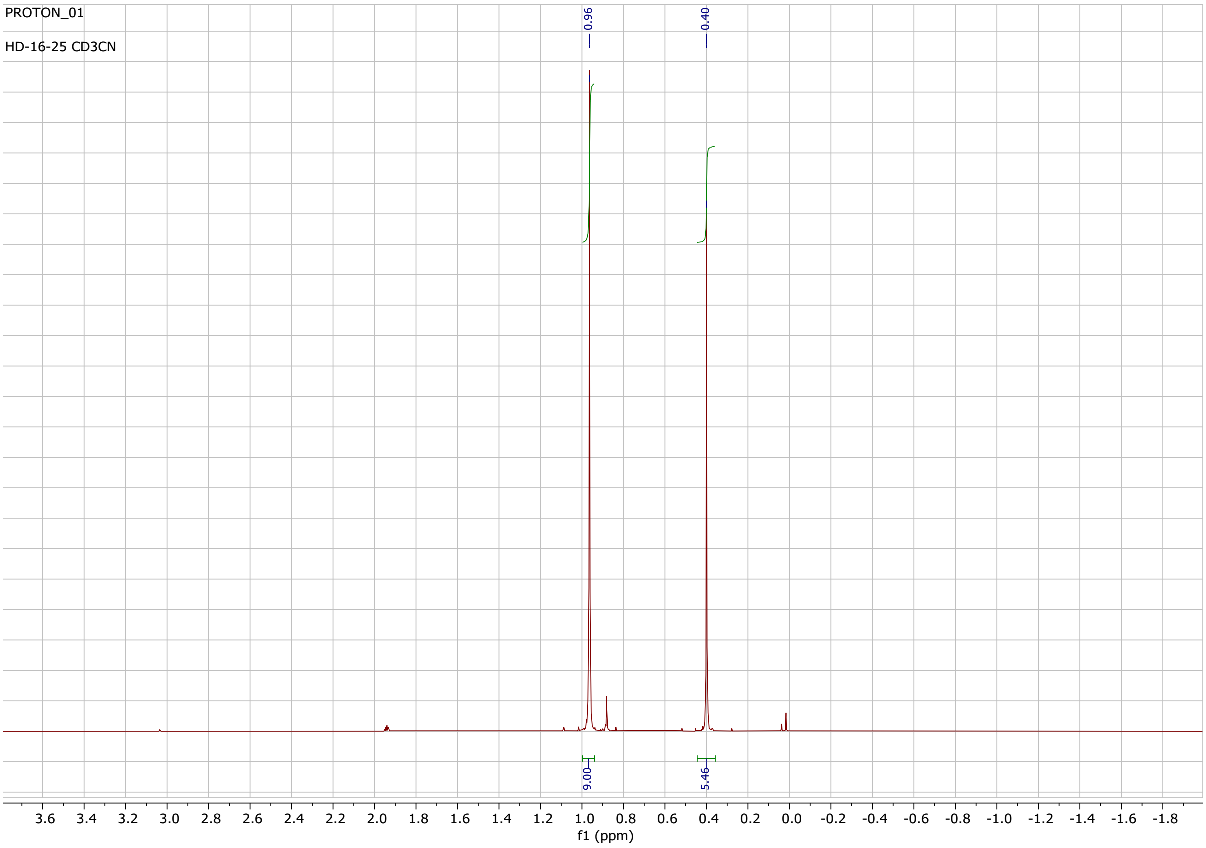

Figure S1: ^{1}H NMR of **1** in CD_3CN.

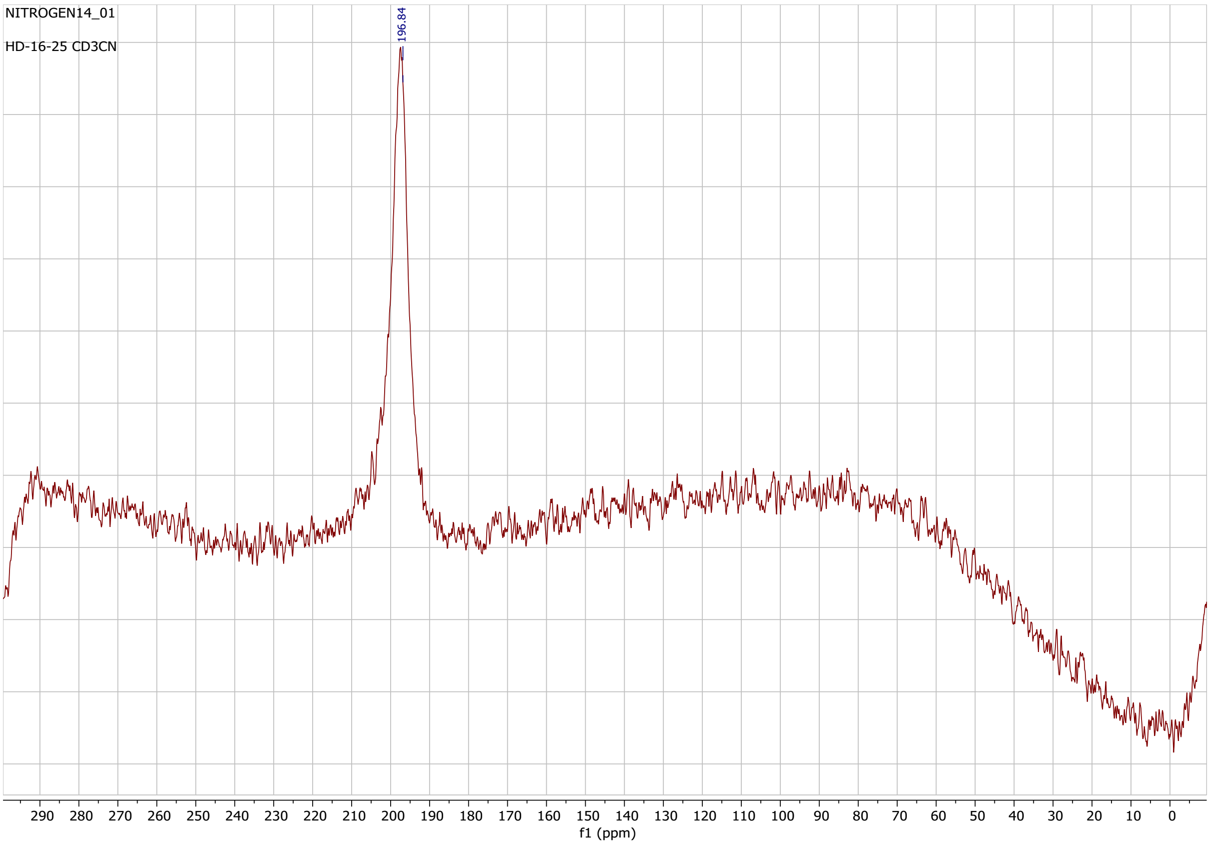

Figure S2: ^{14}N NMR of **1** in CD_3CN.

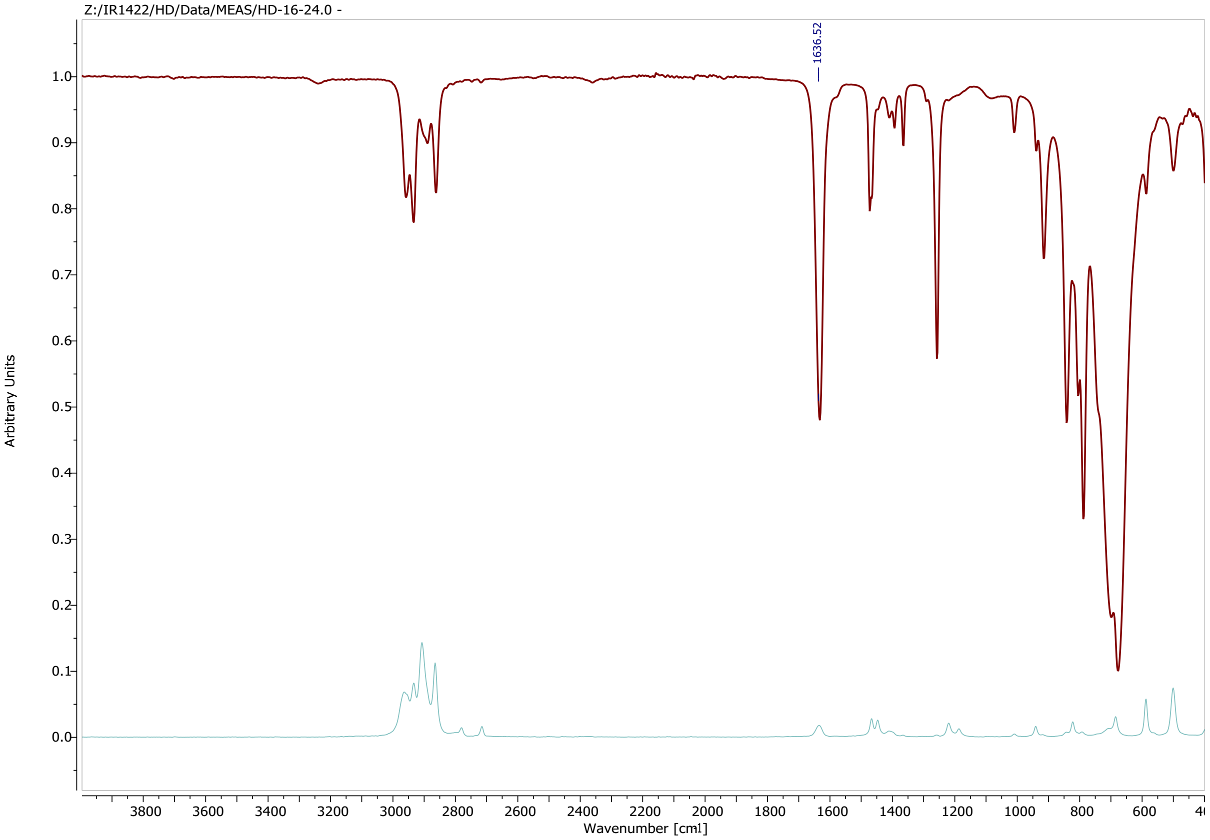

Figure S3: Liquid state IR (top trace) and Raman (bottom trace) of **1**.

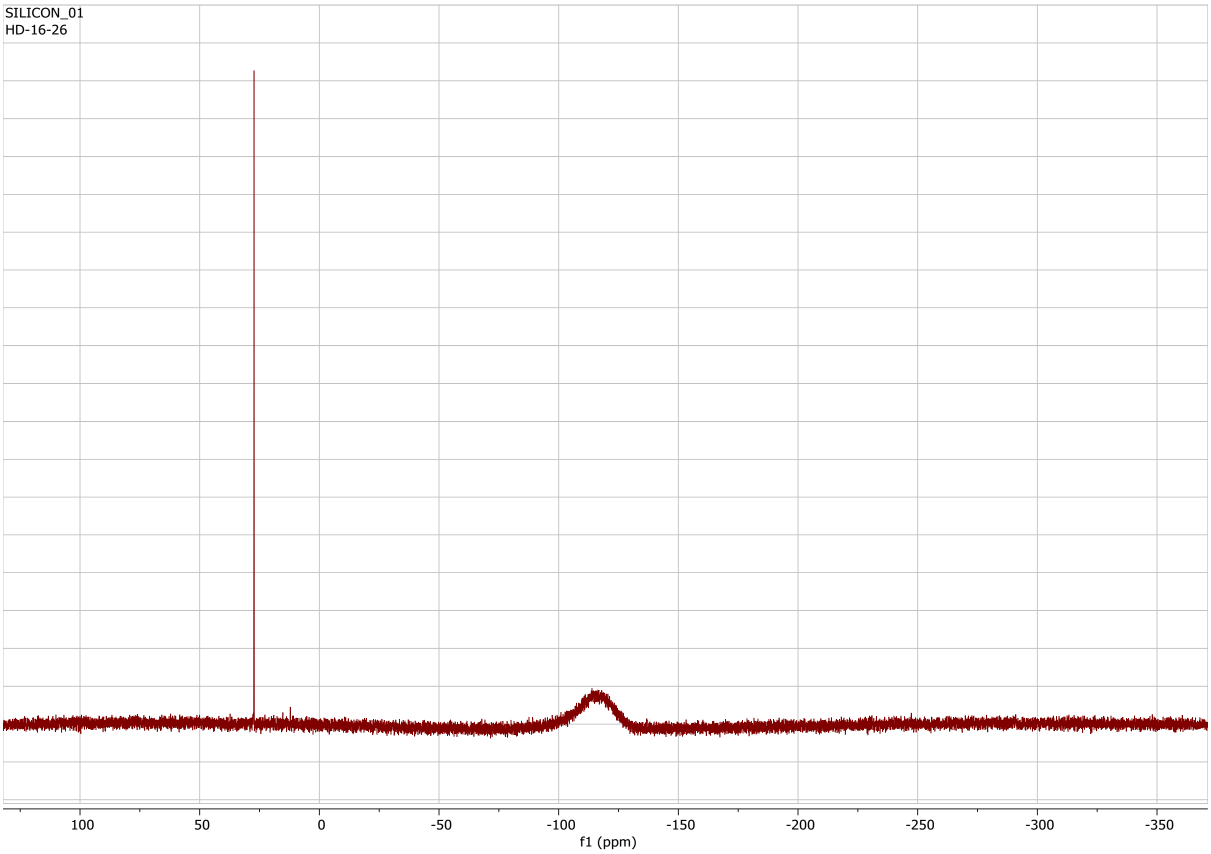

Figure S4: ^{29}Si NMR of **1** in CD_3CN. The broad signal at *ca.* -100 ppm belongs the borosilicates of the sample tube and probe material.

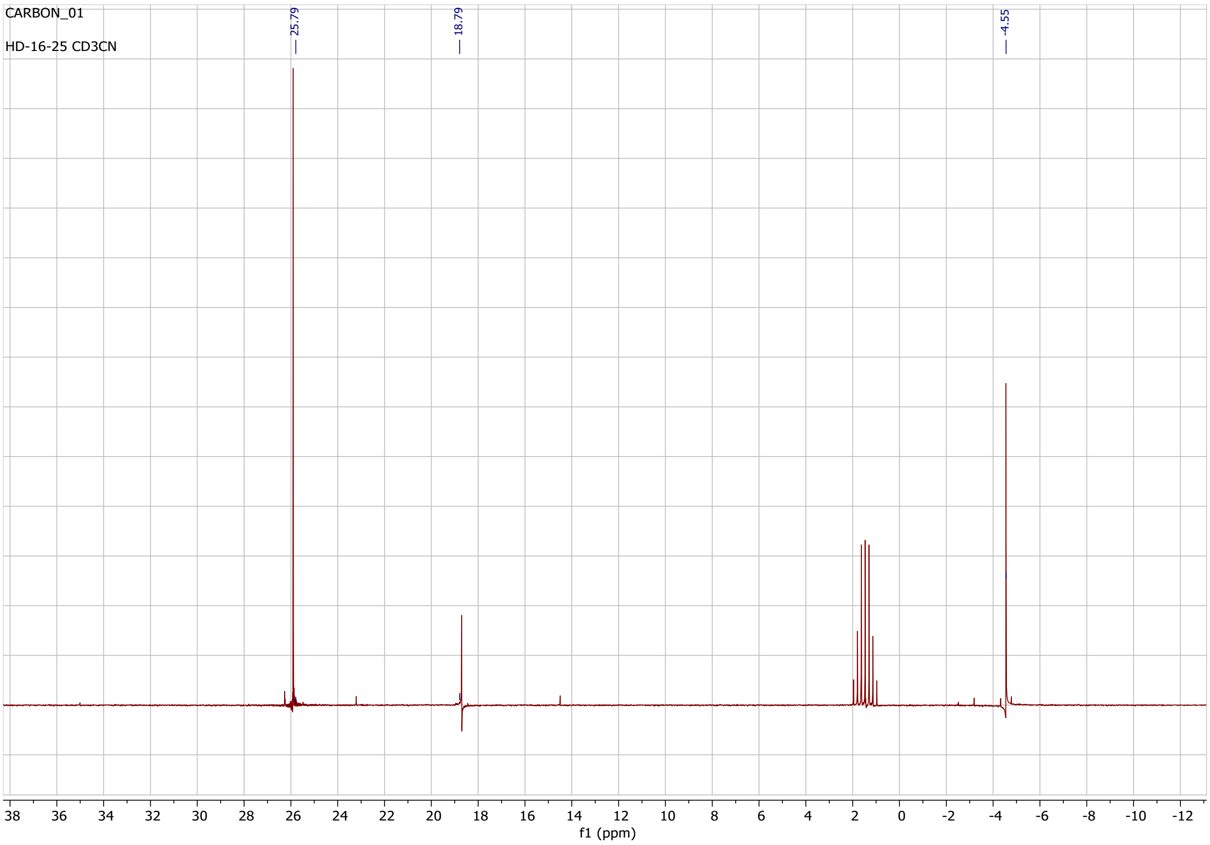

Figure S5: ^{13}C NMR of **1** in CD_3CN.

Synthesis and isolation of tri*i*sopropylnitritosilane (2)

The reaction was conducted on a Schlenk line. A solution of tri*iso*propylsilyl chloride *i*Pr_3SiCl (193 mg, 1.00 mmol) in acetonitrile (2 mL) was cannulated over a silver nitrite (154 mg, 1.00 mmol) solution in acetonitrile (2 mL). The resulting suspension was stirred for 1 h, after which time the silver chloride precipitate was removed by decantation. The solvent from the supernatant solution was removed *in vacuo* over several hours, yielding the compound as a pale-yellow oil.

^{1}H NMR (CH_3CN): δ=1.10 ppm (d, 18H, *CH_3*), δ=1.41 ppm (m, 3H, *CH*)

^{14}N NMR (CH_3CN): δ=198 ppm (s, ONO)

^{13}C{^{1}H} NMR (CH_3CN): δ=12.2 pm (d, 3C, *CH*), δ=17.4 ppm (s, 3C, *CH_3*)

^{29}Si NMR (CH_3CN): δ=21.8 ppm (s, Si)

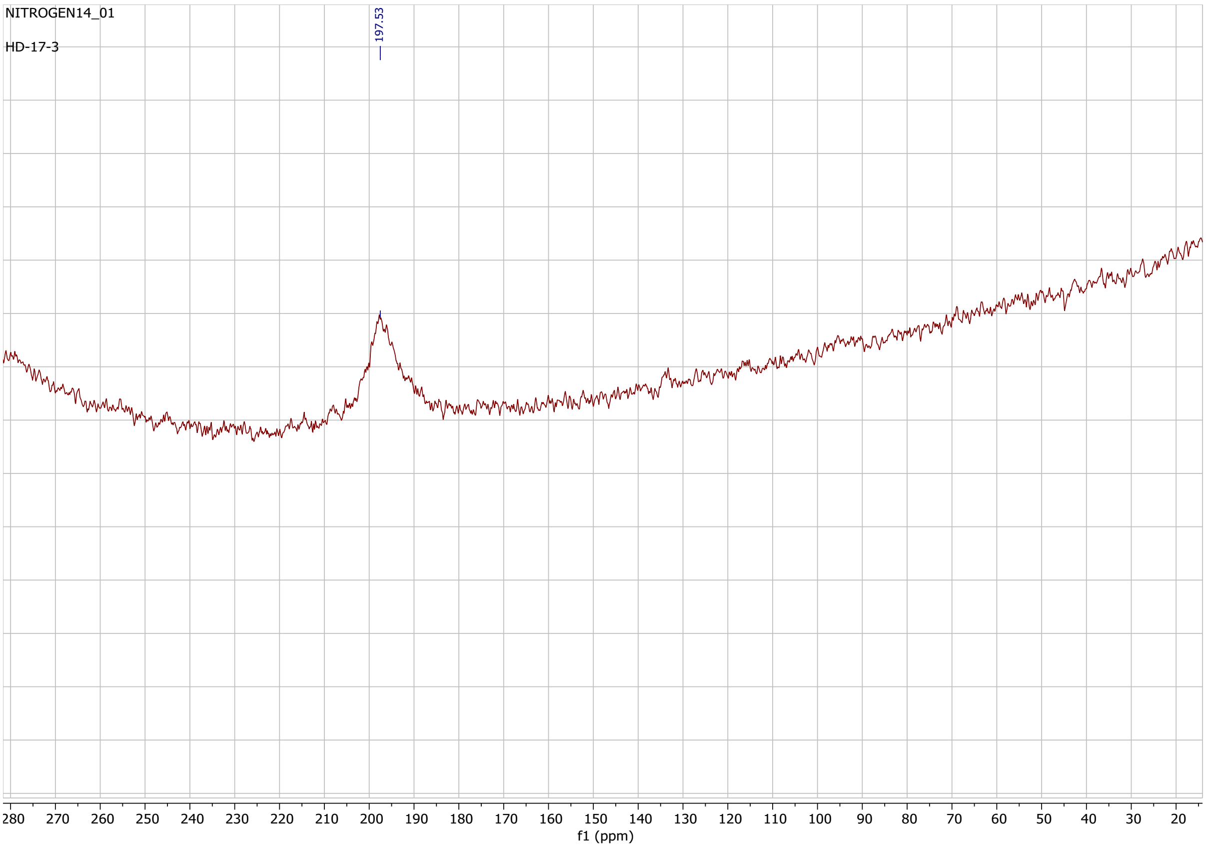

Figure S6: ^{14}N NMR of **2** in CH_3CN (unlocked).

.

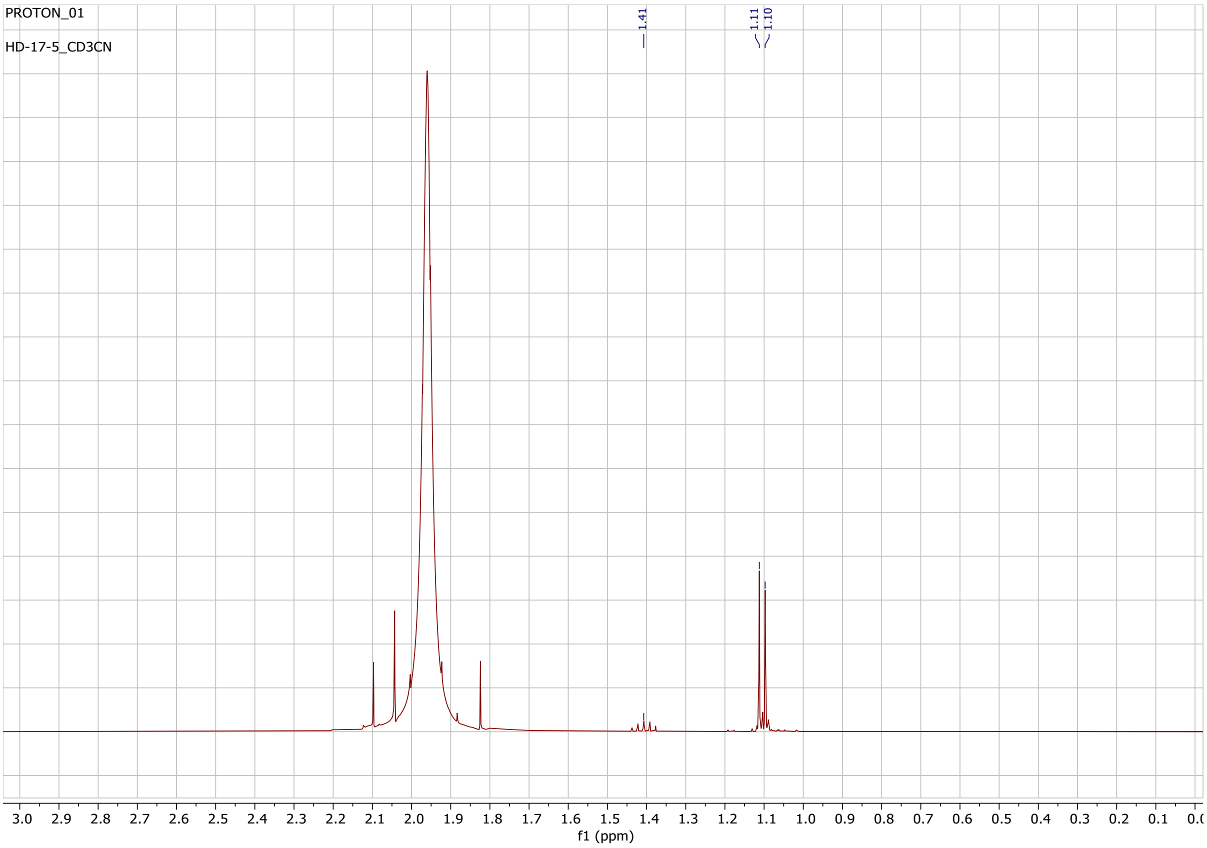

Figure S7: ^{1}H NMR of **2** in CH_3CN (unlocked).

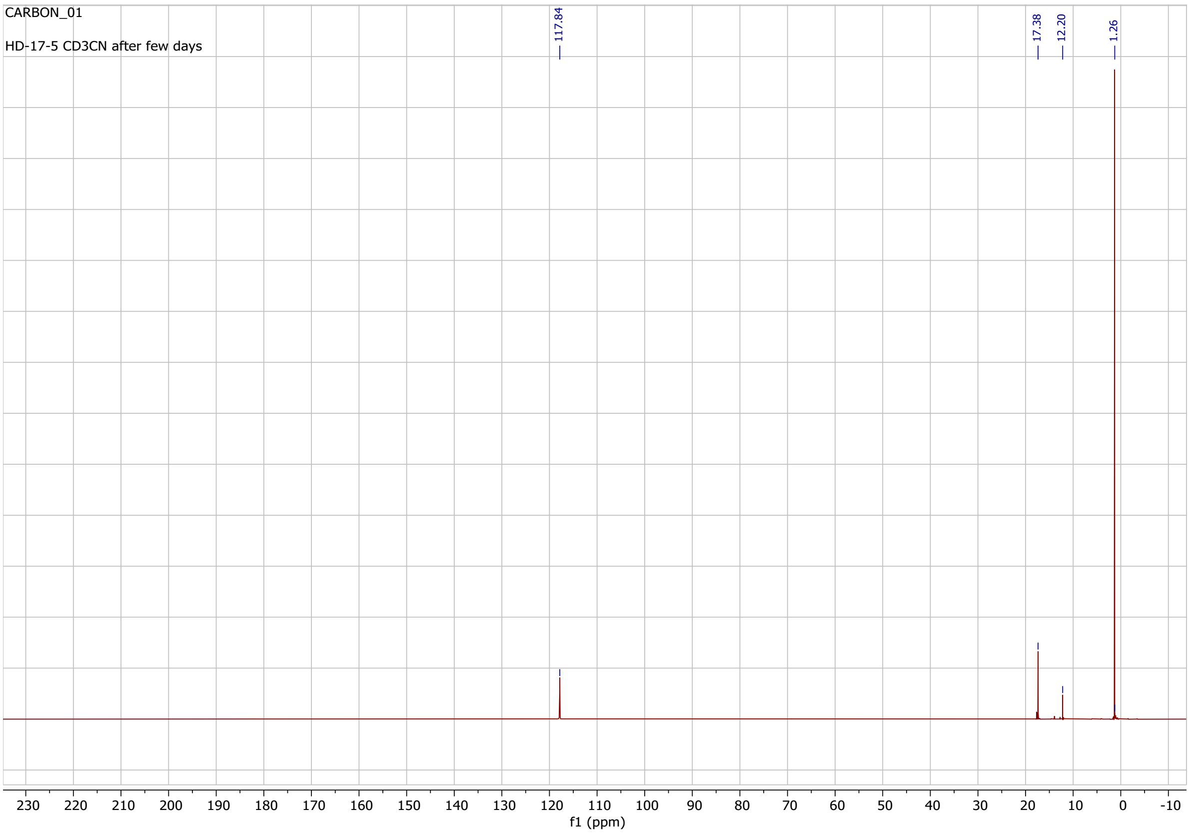

Figure S8: ^{13}C NMR of **2** in CH_3CN (unlocked).

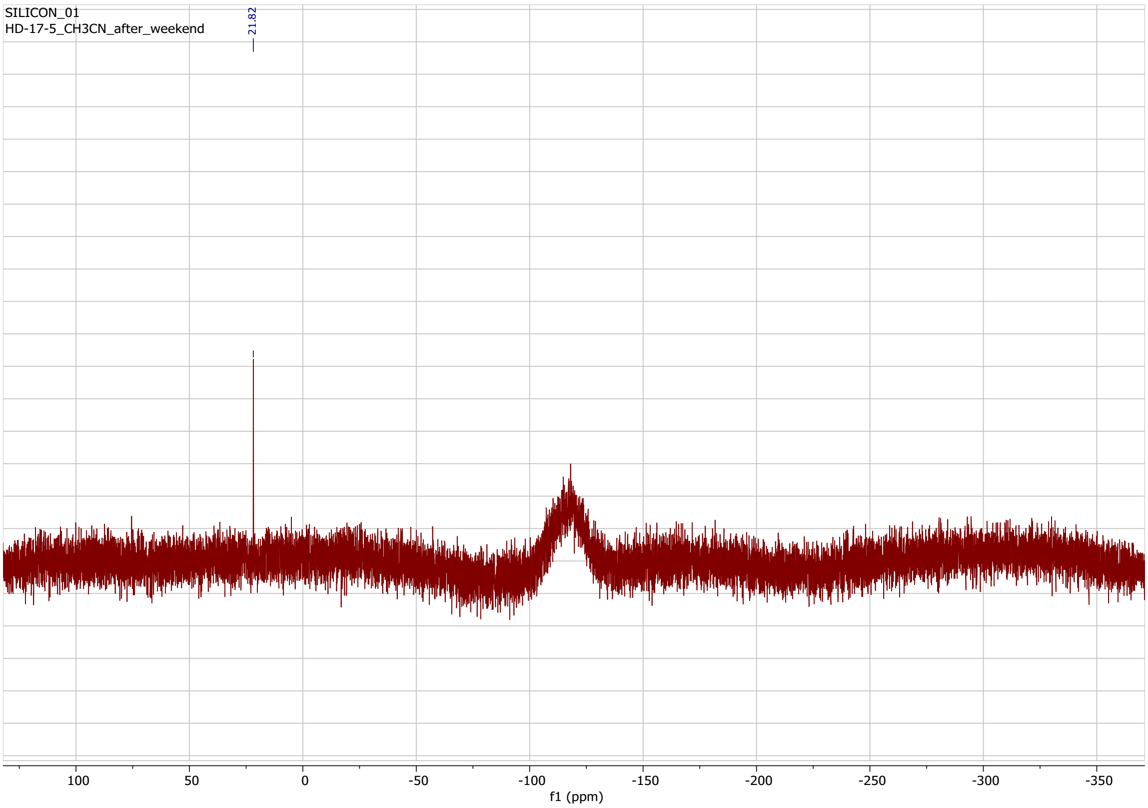

Figure S9: ^{29}Si NMR of **2** in CH_3CN (unlocked). The broad resonance at -120 ppm belongs to the borosilicate glass of the NMR tube and probe.

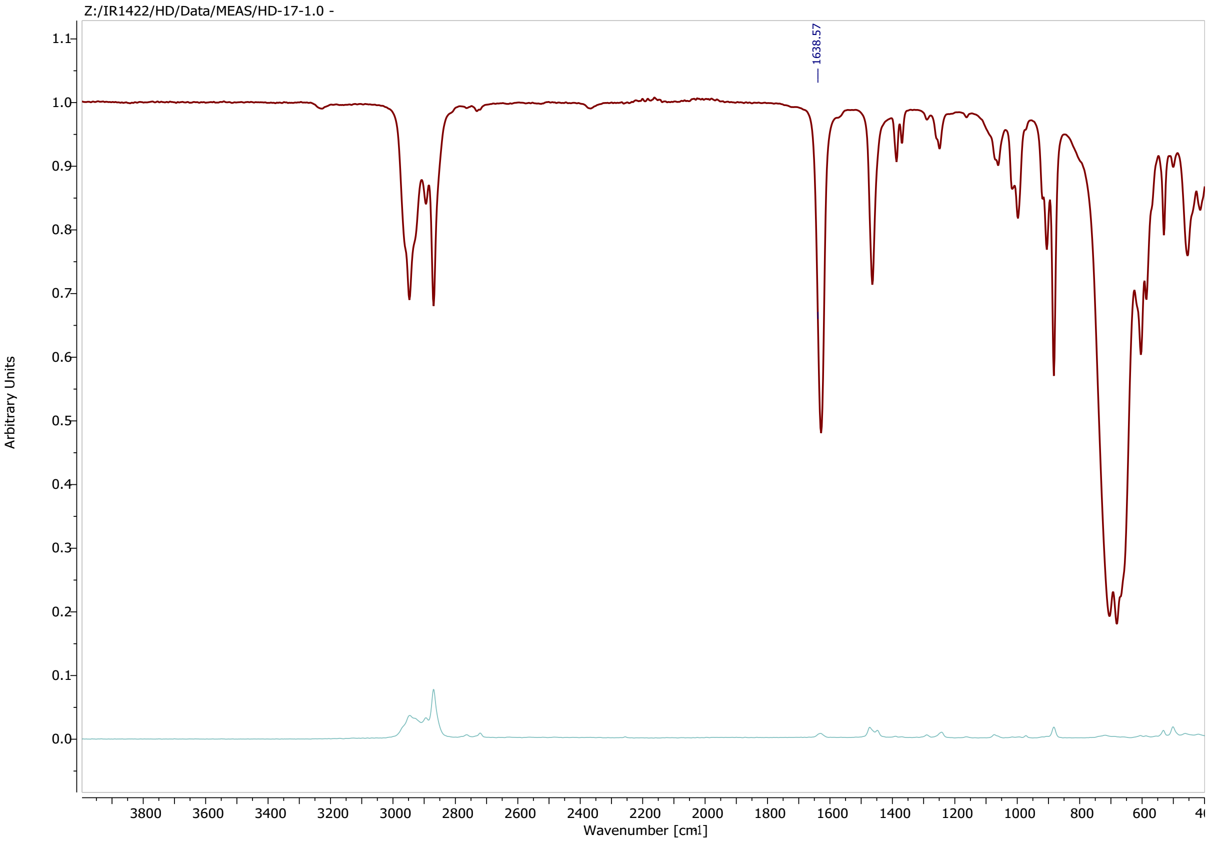

Figure S10: Liquid state IR (top trace) and Raman spectra (bottom trace) of **2**.

Observation of trimethylnitritosilane (3)

Trimethylsilyl chloride (1 eq) was condensed over a dichloromethane suspension of silver nitrite at −196 °C. The mixture was thawed at −96 °C, at which point no obvious decomposition (no color change or gas evolution) had taken place. After slowly warming up to room temperature, a yellow-orange solution was obtained. The volatiles were condensed into a new NMR tube at −196 °C and NMR analysis showed the presence of a covalent nitrite (196 ppm in ^{14}N NMR) and of ClNO (236 ppm in ^{14}N NMR). N_2O_3 is presumably poorly soluble in dichloromethane and its blue color could only be observed when all volatiles were condensed at −196 °C.

^{1}H NMR (dichloromethane): δ=0.40 ppm (s, 9H, *CH$_3$*) for the silyl nitrite

^{14}N NMR (dichloromethane): δ=196 ppm (s, ONO), δ=236 ppm (s, ClNO)

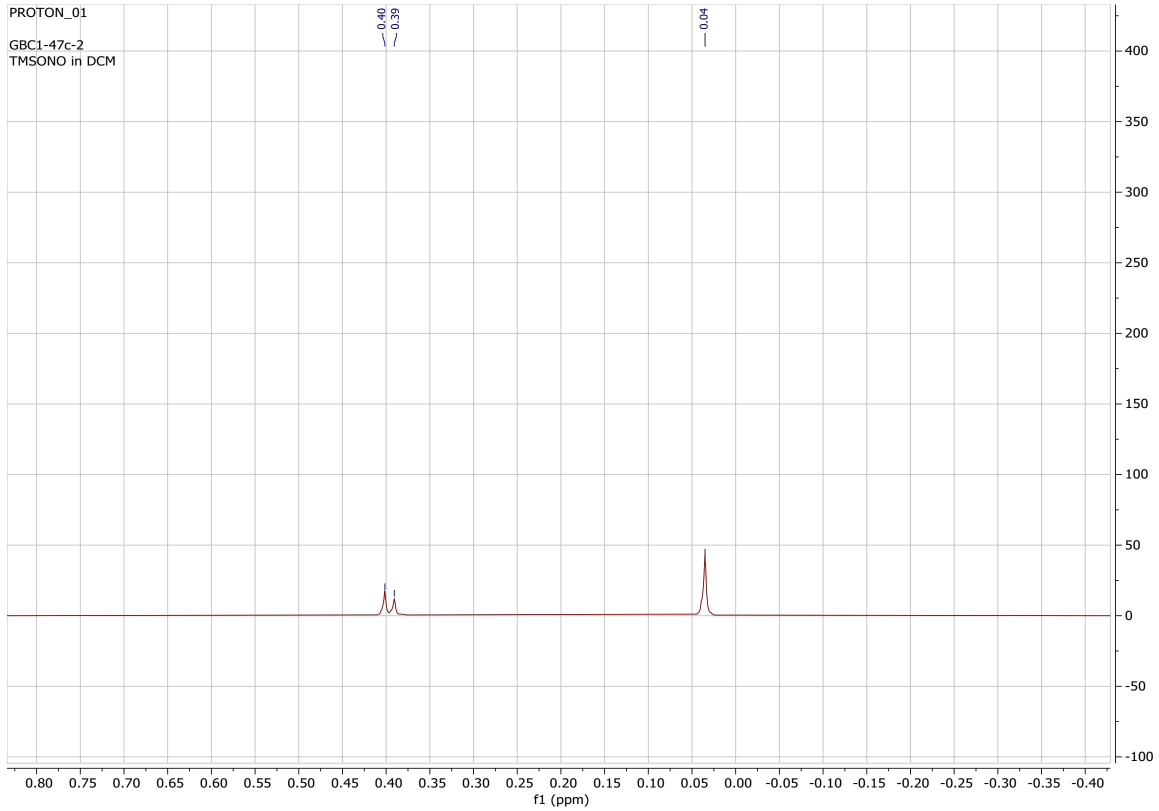

Figure S11: ^{1}H NMR of a mixture containing **3** in dichloromethane (unlocked), δ=0.40 ppm belongs to the silyl nitrite, δ=0.39 for Me_3SiCl and δ=0.04 ppm for hexamethylsiloxane.

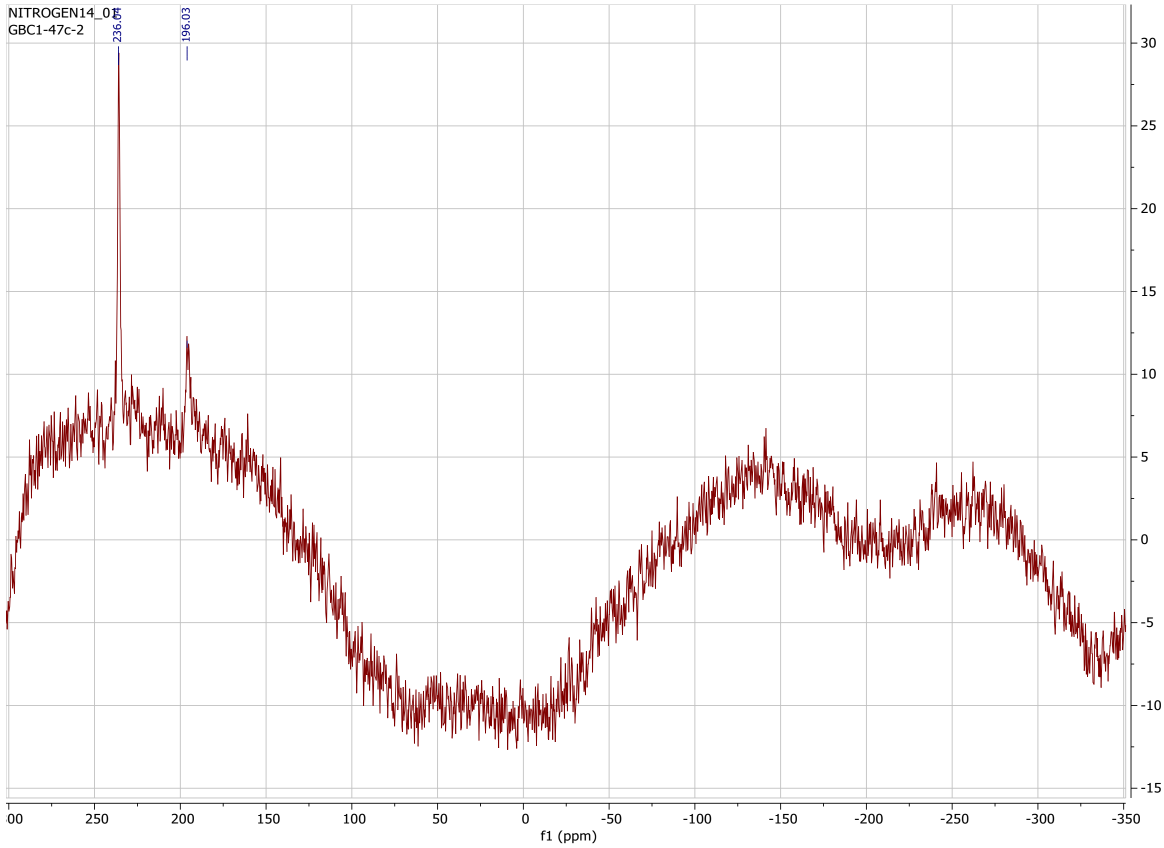

Figure S12: ^{14}N NMR of a mixture containing **3** in dichloromethane (unlocked).

Observation of *tert*-butyldiphenylnitritosilane (4)

*t*BuPh$_2$SiCl (687 mg, 2.50 mmol) and AgNO$_2$ (385 mg, 2.50 mmol) were suspended in acetonitrile (3 mL) in a glass reactor. The mixture was stirred for 2-3 h. After completion, the mixture was filtered in the glovebox using decantation to remove the AgCl. The resulting solution was analyzed by ^{14}N NMR spectroscopy, which indicated the formation of the nitrite. The solvent was removed under vacuum for several hours, yielding a pale-yellow oil. Characterization was performed using NMR, Raman, and IR spectroscopy, and indicated that the compound had already substantially decomposed. The signals attributed to **3** are listed below:

^{14}N NMR (CH$_3$CN): δ=192 ppm (s, ONO)

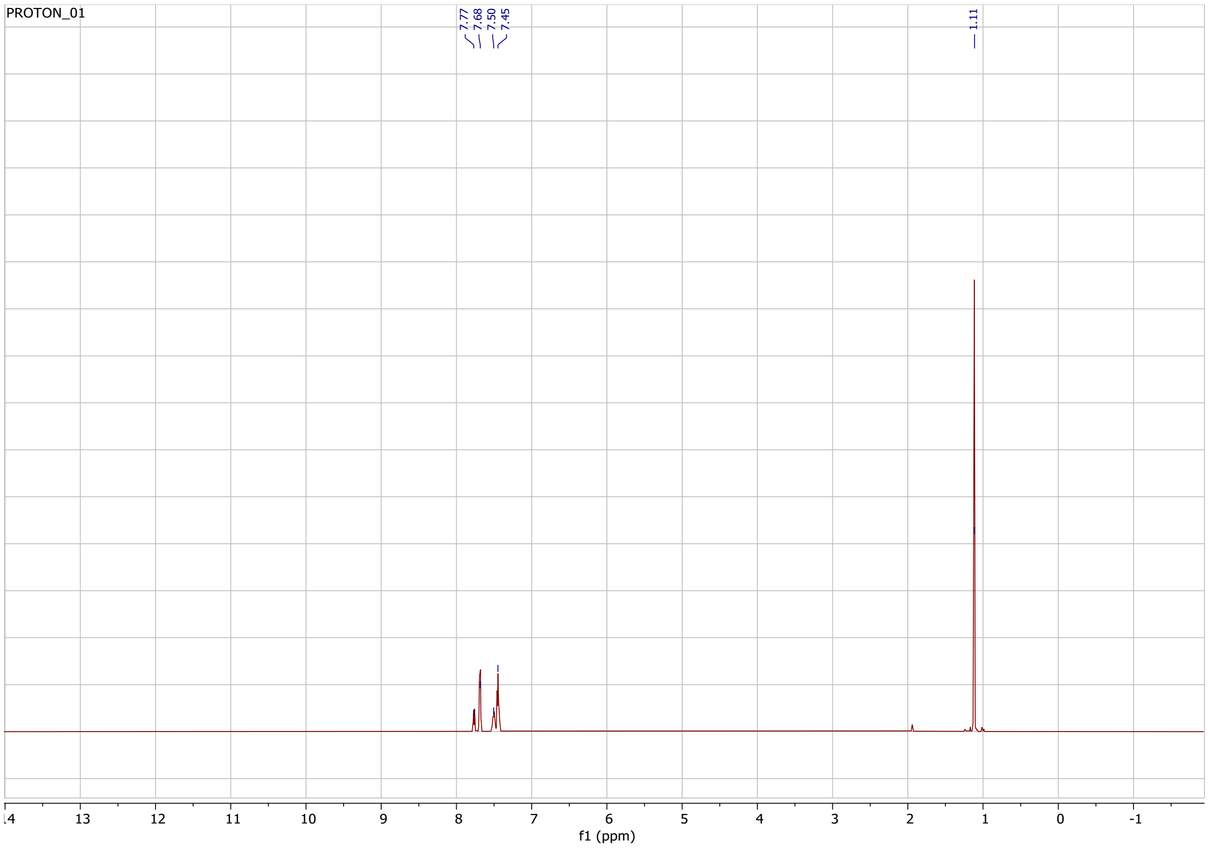

Figure S13: ^{1}H NMR of a mixture containing **4** in CD_3CN.

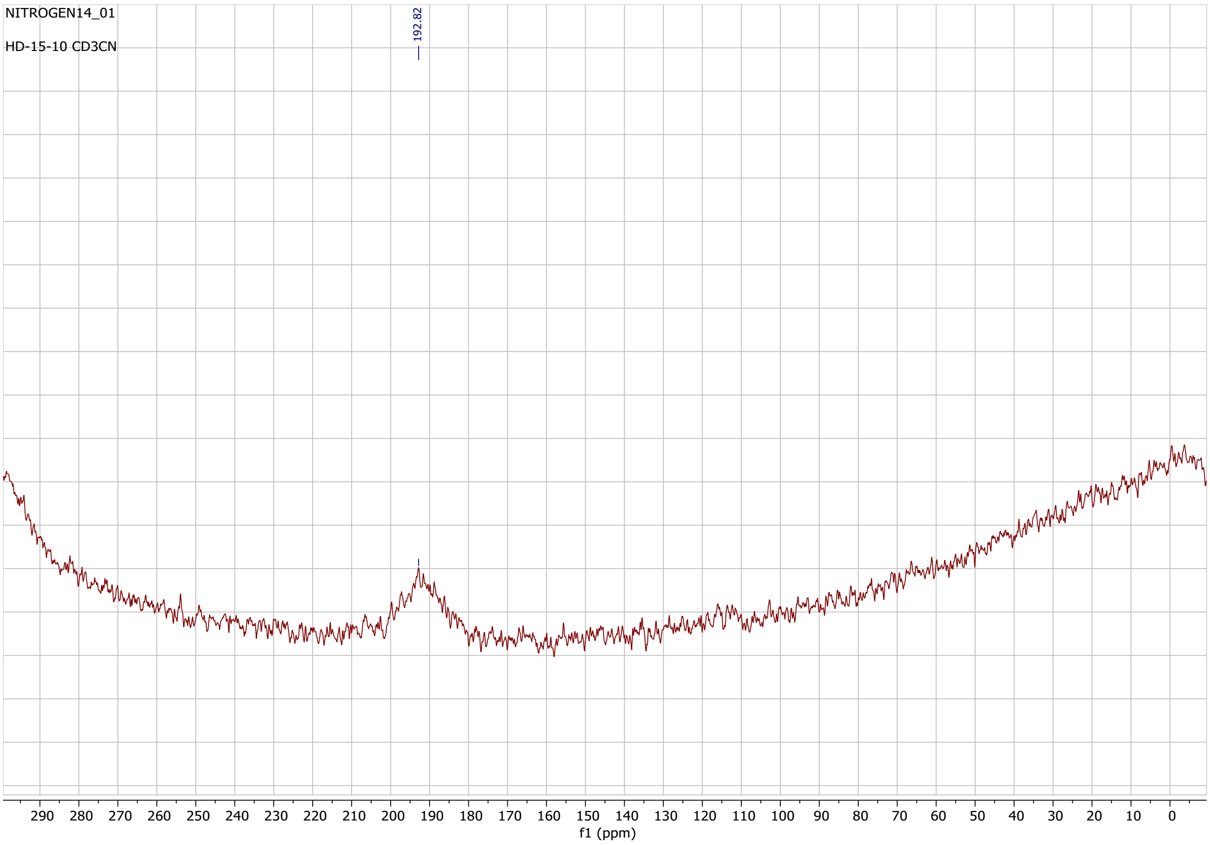

Figure S14: ^{14}N NMR of a mixture containing **4** in CD_3CN.

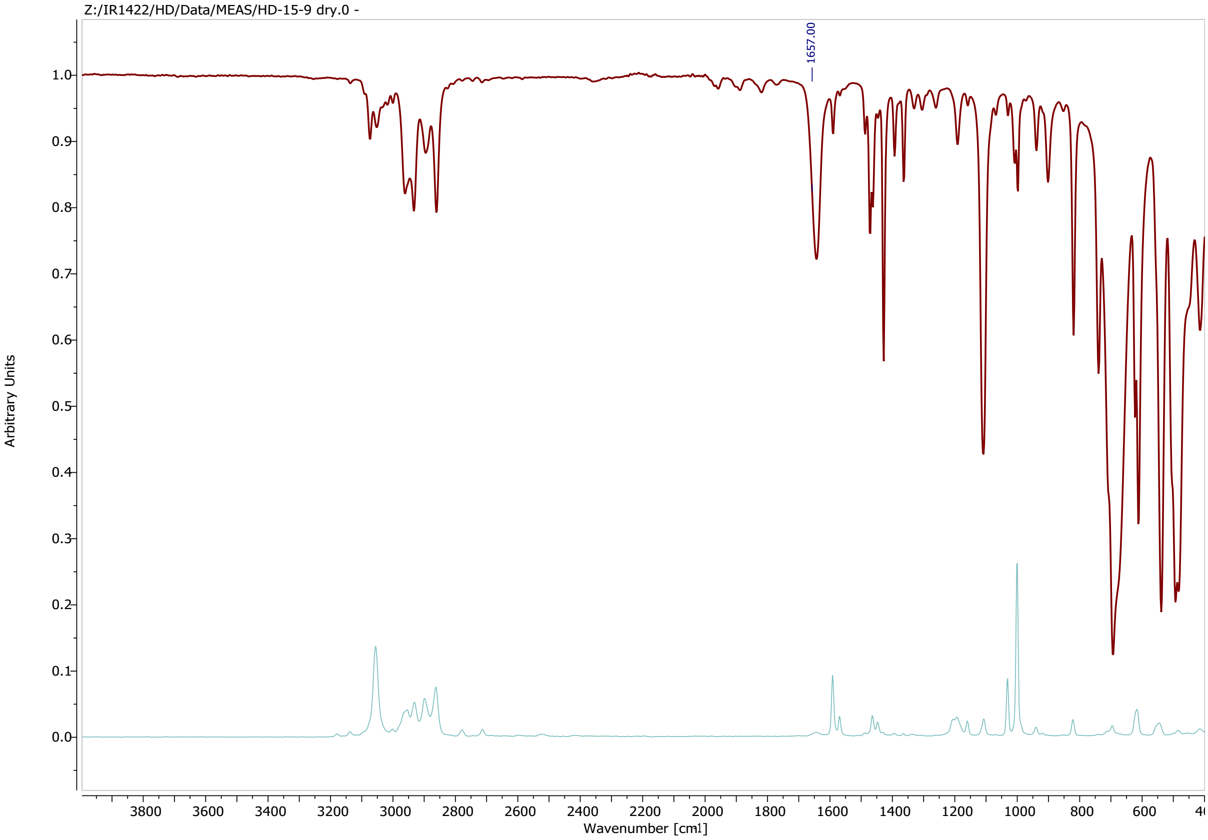

Figure S15: Liquid state IR (top trace) and Raman (bottom trace) of a mixture containing **4**.

Observation of triethoxychloronitritosilane (5)

A solution of triethoxychlorosilane (13 mg; 65 µmol) in acetonitrile was added to a silver nitrite (9 mg; 0.06 mmol) solution in the same solvent. A copious white precipitate formed and rapidly settled. NMR spectroscopy revealed the presence of two species in a ratio 1:1, identified as triethoxynitritosilane and the decomposition product $((EtO)_3Si)_2O$. The silyl nitrite decomposed relatively quickly in solution and had almost entirely converted into the silyl ether within 24 h.

^{1}H NMR (CH_3CN): δ=3.91 ppm (q, 6H, $^{3}J_{H-H}$= 7 Hz, $C\mathit{H}_2$), 1.20 (t, $^{3}J_{H-H}$= 7 Hz, 9H, $C\mathit{H}_3$).

^{14}N NMR (CH_3CN): δ=183 ppm (s, O*N*O)

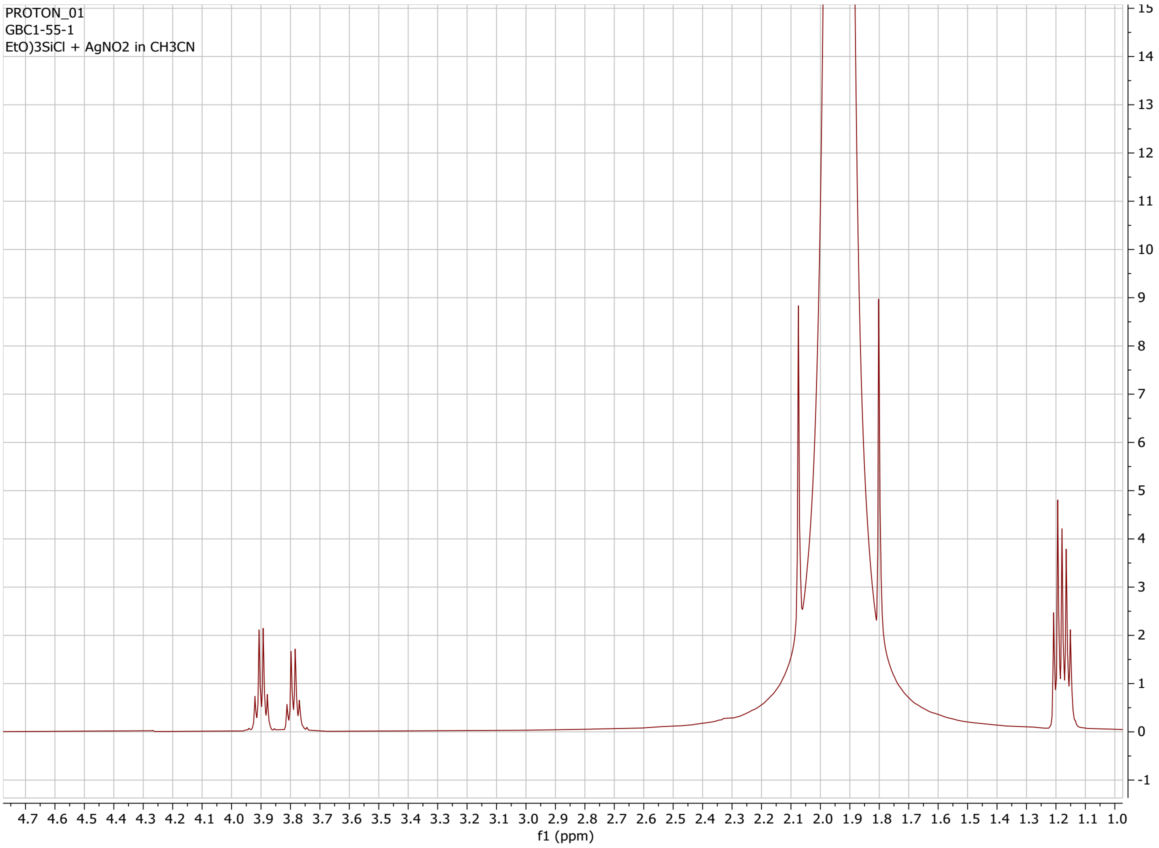

Figure S16: ^{1}H NMR spectrum in CH_3CN (unlocked) showing **5** and its silyl ether decomposition product. The multiplet at 1.15 results from the overlap of the two triplets due to the two species.

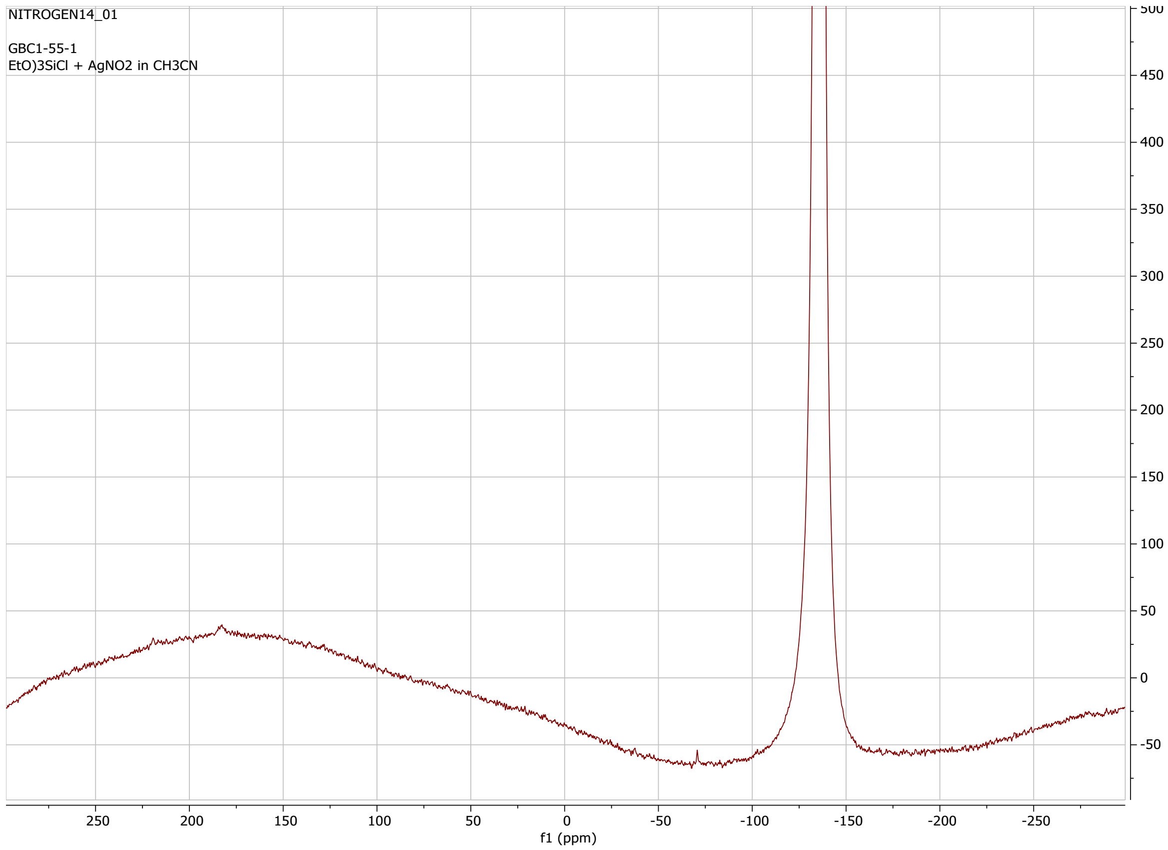

Figure S17: ^{14}N NMR spectrum in CH_3CN (unlocked) showing **5** as a very weak signal at 183 ppm. This signal decreases and then disappears within 24 h. The weak signal at -71 ppm belongs to dissolved N_2.

Observation of triphenylnitritosilane (6)

Ph_3SiCl (88.5 mg, 0.300 mmol) and $AgNO_2$ (46.2 mg, 0.300 mmol) were placed in 1.5 mL dichloromethane. The reaction was carried out in a glove box, where the mixture was stirred at room temperature for 2 h. Analysis by ^{14}N NMR revealed a broad signal around 185 ppm, suggesting the formation of the desired nitrite. Further characterization by IR spectroscopy showed a rather intense band around 1600 cm^{-1}, supporting the presence of the ONO group. NMR analysis showed that at least two to three species were present in the isolated mixture, indicating partial conversion and decomposition.

A crystallization attempt was carried out by transferring a portion of the reaction supernatant without fully drying off the dichloromethane into a small vial. Two drops of pentane were added, and the vial was placed inside a larger vial containing additional pentane to enable vapor diffusion. The larger vial was then sealed and stored at –20 °C under inert atmosphere. Transparent crystals formed along with a few yellowish crystals and the former were analysed by X-ray diffraction (see below). The crystals slowly become yellow and opaque once exposed to ambient air.

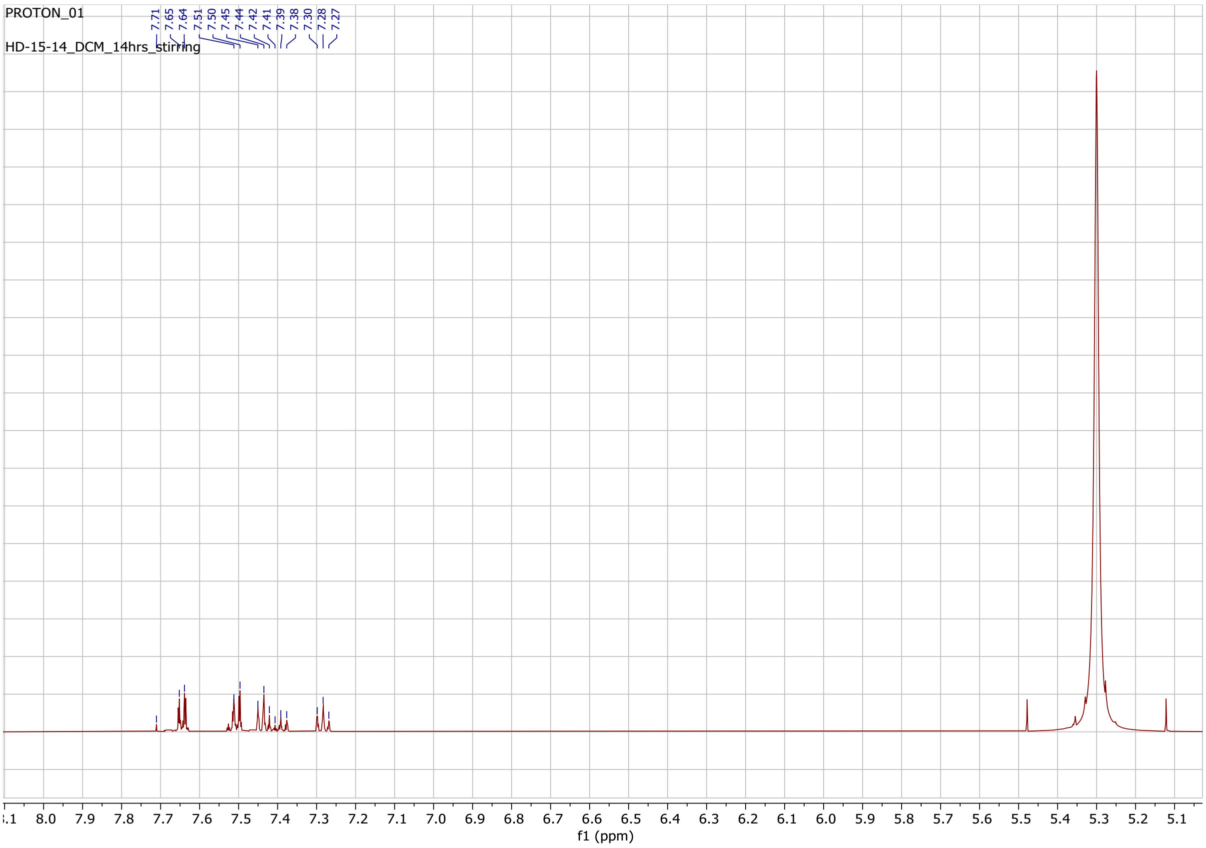

Figure S18: ^{1}H NMR of a mixture containing **6** in dichloromethane (unlocked).

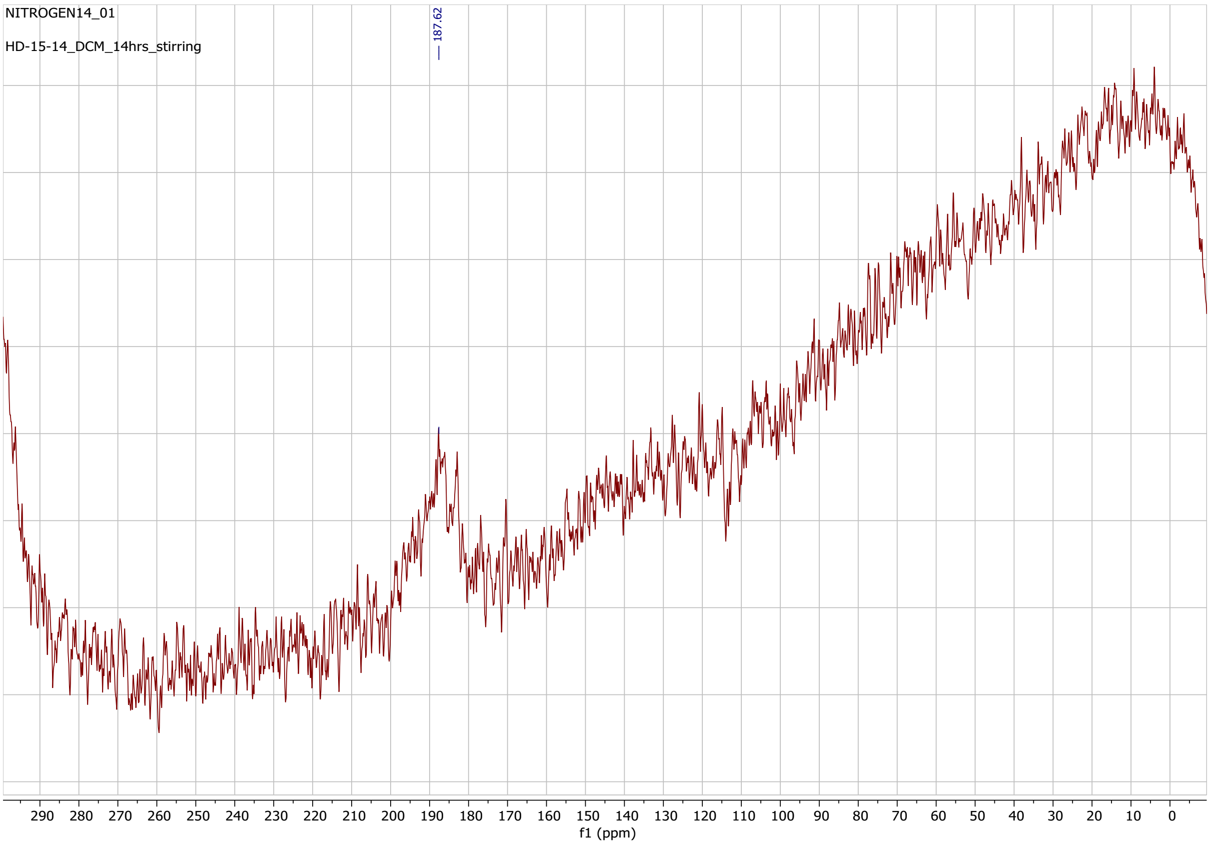

Figure S19: ^{14}N NMR of a mixture containing **6** in dichloromethane (unlocked)

Observation of phenyldimethylnitritosilane (7):

$AgNO_2$ and $PhMe_2SiCl$ were weighed separately in two J.Y.-style NMR tubes, and the chloride was cannulated onto $AgNO_2/CH_3CN$. Immediately upon mixing, a blue color appeared, which gradually shifted to a yellowish orange, indicating the formation of NO_2. No signal could be observed by ^{14}N NMR analysis of the resulting mixture. ^{1}H NMR only showed decomposition products, including the formation of the silyl ether with a signal around $\delta=0.04$ ppm, confirming rapid decomposition in acetonitrile at room temperature.

The same reaction was subsequently attempted in dichloromethane at the 300 μmol scale. This time, a nitrite signal was detected around $\delta = 192$ ppm in the ^{14}N NMR spectrum, indicating partial formation of the desired product. However, a signal at $\delta \approx 230$ ppm attributable to ClNO was also observed, consistent with the reaction of the silyl chloride starting material with the slowly forming silyl nitrite.

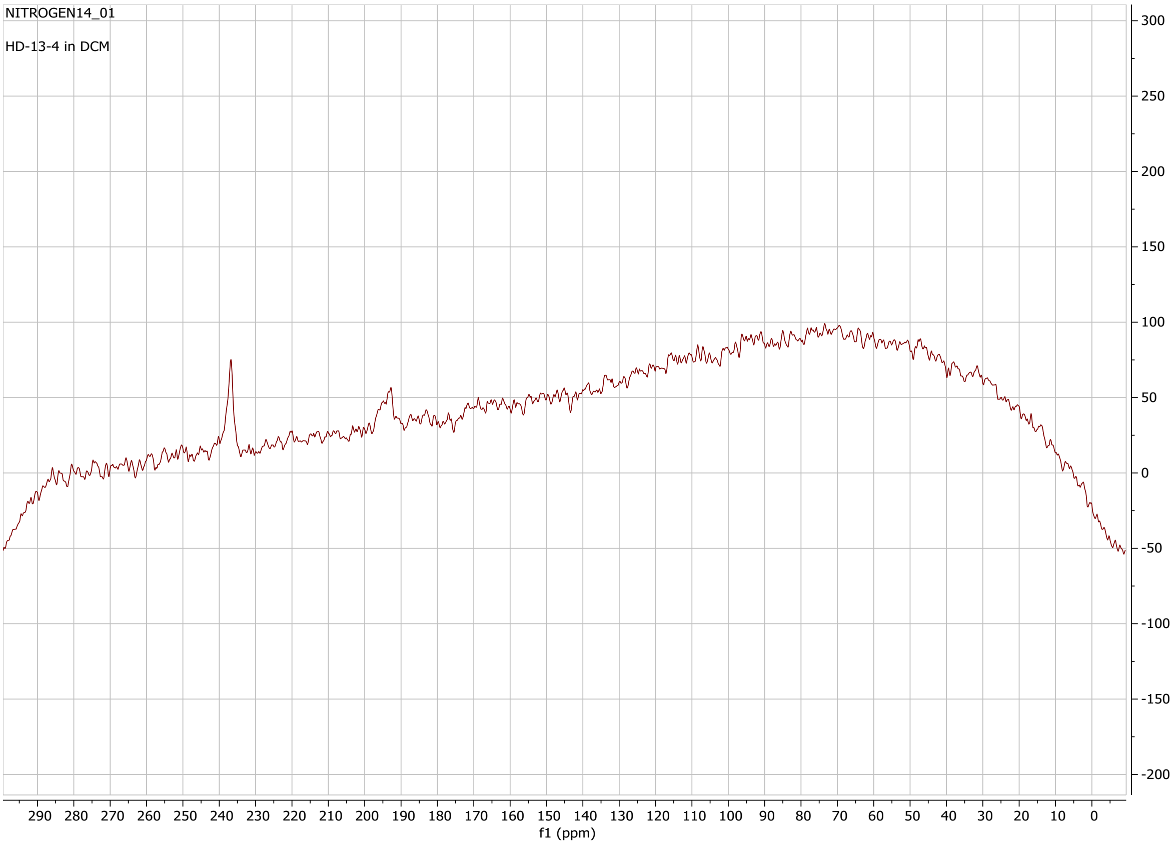

Figure S20: ^{14}N NMR of a mixture containing **7** in dichloromethane (unlocked).

Stability of 1

Tert-Butyldimethylsilyl nitrite was found to be moderately stable in acetonitrile solution at room temperature. No significant changes were observed within the first few days; however, signs of decomposition became evident after one week. By the four-week mark, approximately 50% of the compound had converted to the corresponding silyl ether, as confirmed by ^{1}H NMR spectroscopy. Thermal stability tests showed that heating to 50°C for 9 h lead to approximately 30% decomposition. Heating to 90°C for 15 mins made the solution turn greenish/yellow and, after 1 h, most of the *tert*-butyldimethylsilyl nitrite turned into the corresponding silyl ether.

Stability of 2

Tri*i*sopropyl silyl nitrite showed excellent stability in solution at room temperature. After two weeks in a sealed J.Y.-style NMR tube under inert atmosphere, negligible decomposition was observed. The neat compound also remained stable for weeks at –20 °C, making it the most robust nitrosilane in this study.

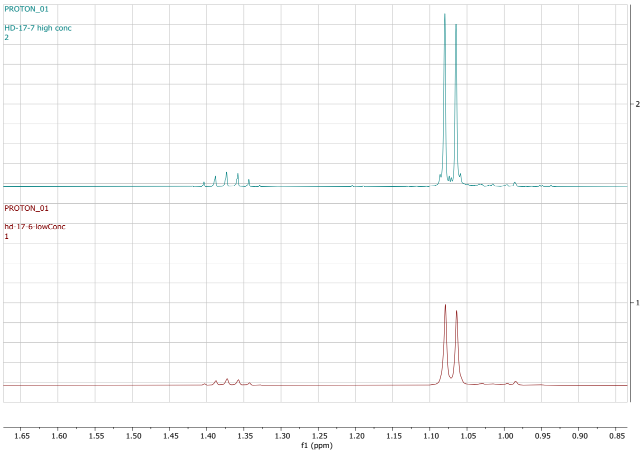

Figure S21: Two samples of **2** in acetonitrile after 2 weeks at room temperature, showing no obvious decomposition.

Computational details

All calculations were performed at the B3LYP/6-311+g(d,p) level of theory using the Gaussian 16, Revision B.01 suite of programs.[1] Solvation effects were approximated using the SMD model, with acetonitrile as the solvent. Unless otherwise mentioned, all predicted values are for acetonitrile solutions. Frequency calculations were performed to confirm that structures are minima on the PES. Vibrational frequencies are reported uncorrected. Gaussian output (.log) files were deposited on the Borealis data repository and are available at: https://doi.org/10.5683/SP3/LQ7JKU

We verified, on two representative systems (H_3Si and tBu_3Si), that our predictions were consistent whether B3LYP or more modern functionals were used and found that values vary by *ca* ± 1 kcal/mol depending on the functional.

Table S1: sample thermochemical and activation energy data for three DFT functionals (in kcal/mol). Solvation effects were approximated with the SMD model (acetonitrile).

	B3LYP				**Wb97xd**				**CAM-B3lyp**			
Species	ΔH_{isom}	ΔG_{isom}	ΔH^{TS}	ΔG^{TS}	ΔH_{isom}	ΔG_{isom}	ΔH^{TS}	ΔG^{TS}	ΔH_{isom}	ΔG_{isom}	ΔH^{TS}	ΔG^{TS}
H_3SiNO_2	-10.5	-11.3	17.0	18.0	-10.3	-10.5	16.9	17.9	-11.5	-11.8	17.2	18.2
tBu_3SiNO_2	-11.2	-11.7	16.5	16.2	-10.4	-10.9	17.1	17.7	-12.1	-12.5	16.7	16.8

^{14}N NMR chemical shift prediction was performed using a parameterized relationship from experimentally-determined chemical shifts (nitrite, 237 .6; nitrate, −1; N_2, −70.7; acetonitrile, −136.1; N_2O, −146.5 and −230.4 ppm) and their computed values, yielding a calibration curve with fitted equation 0.9108x+10.129 with R^2= 0.9987.

All computed shielding values are referenced by subtracting them to the shielding value predicted for nitromethane (−169.833 ppm). The referenced value is then entered into the following formula:

(Referenced value x 0.91089) + 10.129 = predicted value

Table S2: Thermochemical and activation energy data for the isomerisation of nitrosilanes into their nitrite analogue.

	Gas phase				**CH_3CN solution**			
Nitrosilane	ΔH^{TS}_{isom}	ΔG^{TS}_{isom}	ΔH_{isom}	ΔG_{isom}	ΔH^{TS}_{isom}	ΔG^{TS}_{isom}	ΔH_{isom}	ΔG_{isom}
H_3SiNO_2	14.4	15.4	−14.6	−15.1	17.0	18.0	−10.5	−11.3
Cl_3SiNO_2	11.0	11.9	−21.9	−22.9	12.0	11.4	−20.7*	−20.4*
F_3SiNO_2	6.0	7.2	−26.0	−27.1	6.6	8.6	−25.6*	−24.3*
$(Me_3Si)_3SiNO_2$	19.8	19.8	−7.3	−8.1	20.5	19.9	−4.9	−5.9
$(MeO)_3SiNO_2$	13.0	14.9	−15.7	−16.2	14.6	16.7	−12.9	−12.7
$(NMe_2)_3SiNO_2$	14.8	16.5	−13.3	−13.7	17.1	17.6	−9.6	−11.1
Me_3SiNO_2	16.6	17.5	−12.5	−12.7	18.7	19.9	−8.6	−8.1
Ph_3SiNO_2	14.9	16.0	−13.8	−14.5	17.1	17.6	−10.5	−11.2
***i*Pr_3SiNO_2**	17.1	17.7	−12.0	−12.5	18.3	18.2	−9.0	−9.8
***t*$BuMe_2SiNO_2$**	16.4	17.3	−12.7	−13.0	18.4	19.1	−8.6	−9.1
***t*Bu_3SiNO_2**	15.7	15.9	−13.8	−14.3	16.5	16.2	−11.2	−11.7

*Nitrites not stable minima in solution

Table S3: Predicted ^{14}N NMR chemical shifts for nitritosilanes (referenced to nitromethane).

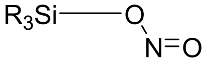

Compound	Predicted chemical shift δ (ppm)
H_3Si	207
Cl_3Si	*
F_3Si	*
$(Me_3Si)_3Si$	227
$(MeO)_3Si$	203
$(NMe_2)_3Si$	221
Me_3Si	220
Ph_3Si	217
iPr_3Si	222
t$BuMe_2Si$	220
tBu_3Si	227

*Nitrites not stable minima in solution

Table S4: Predicted ^{14}N NMR chemical shifts for nitrosilanes (referenced to nitromethane).

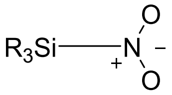

Compound	Predicted chemical shift δ (ppm)
H_3Si	56
Cl_3Si	35
F_3Si	24
$(Me_3Si)_3Si$	83
$(MeO)_3Si$	60
$(NMe_2)_3Si$	82
Me_3Si	80
Ph_3Si	73
iPr_3Si	80
t$BuMe_2Si$	78
tBu_3Si	74

Table S5 : Selected predicted bond distances (in Å) for the hypothetical nitritosilanes investigated.

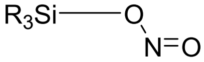

Compound	Si-O	O-N	N=O
H_3Si	1.733	1.412	1.173
Cl_3Si	1.637*	1.636*	1.125*
F_3Si	1.618*	1.667*	1.119*
$(Me_3Si)_3Si$	1.800	1.370	1.189
$(MeO)_3Si$	1.710	1.421	1.171
$(NMe_2)_3Si$	1.769	1.372	1.188
Me_3Si	1.769	1.377	1.185
Ph_3Si	1.752	1.395	1.179
iPr_3Si	1.777	1.372	1.188
t$BuMe_2Si$	1.769	1.376	1.186
tBu_3Si	1.773	1.375	1.187

*Nitrites not stable minima in solution

Table S6: Selected predicted bond distances (in Å) for the hypothetical nitrosilanes investigated.

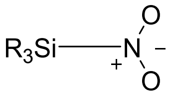

Compound	Si-N	N=O (average of two)
H_3Si	1.903	1.230
Cl_3Si	1.900	1.224
F_3Si	1.853	1.225
$(Me_3Si)_3Si$	1.942	1.235
$(MeO)_3Si$	1.906	1.232
$(NMe_2)_3Si$	1.970	1.235
Me_3Si	1.933	1.233
Ph_3Si	1.941	1.232
iPr_3Si	1.950	1.234
t$BuMe_2Si$	1.934	1.234
tBu_3Si	1.958	1.233

Table S7: Predicted NO stretch frequencies for nitritosilanes.

Compound	$\nu_{N=O}$ (cm^{-1})
H_3Si	1722
Cl_3Si	1957*
F_3Si	1994*
$(Me_3Si)_3Si$	1641
$(MeO)_3Si$	1729
$(NMe_2)_3Si$	1646
Me_3Si	1666
Ph_3Si	1690
iPr_3Si	1651
t$BuMe_2Si$	1663
tBu_3Si	1652

*Nitrites not stable minima in solution

Table S8: Predicted NO_2 stretch frequencies for nitrosilanes.

Compound	$\nu_{ONOasym}$ (cm^{-1})	ν_{ONOsym} (cm^{-1})
H_3Si	1498	1409
Cl_3Si	1542	1392
F_3Si	1539	1408
$(Me_3Si)_3Si$	1461	1371
$(MeO)_3Si$	1496	1417
$(NMe_2)_3Si$	1457	1401
Me_3Si	1478	1412
Ph_3Si	1485	1403
iPr_3Si	1468	1403
t$BuMe_2Si$	1469	1405
tBu_3Si	1464	1397

X-ray crystallography

Crystals of X-ray diffraction quality were grown from a dichloromethane solution at -30 °C.

The crystal data for Ph_3SiONO (**6**) were collected on a RIGAKU XTALAB MINI equipped with a HyPix Bantam hybrid photon counting detector and a Shine high intensity curved monochromator and using Mo Kα (λ = 0.71073 Å) radiation. The data was processed using the CrysAlis^{PRO} software suite. The structure was solved using the intrinsic phasing method,[2] refined with the SHELXL[3] and OLEX[4] programs and expanded using Fourier techniques. All non-hydrogen atoms were refined anisotropically. Hydrogen atoms were included in structure factor calculations. All hydrogen atoms were assigned to idealized geometric positions and depicted (unless otherwise mentioned) as spheres of arbitrary radius. Ellipsoids are represented at the 50% probability level. Beige = silicon, blue = nitrogen, red=oxygen, dark grey = carbon.

Crystallographic data have been deposited with the Cambridge Crystallographic Data Center as supplementary publication number CCDC 2469460. These data can be obtained free of charge from The Cambridge Crystallographic Data Centre *via* www.ccdc.cam.ac.uk/data_request/cif

As expected from *in situ* NMR spectroscopic characterizations, Ph_3SiONO is expected to be found along with unreacted Ph_3SiCl starting material. The crystal was indeed found to contain some chloride, treated as a substitutional chloro : nitrite disorder with refined ratios of 0.15: 0.85. Note that the refined parameters, without any restraint, yield sensible Si-O, Si-Cl, and N-O bond distances, rather close to the predicted values. The size and shape of the O and N ellipsoids is consistent with a conformational disorder in the nitrite group (not modeled).

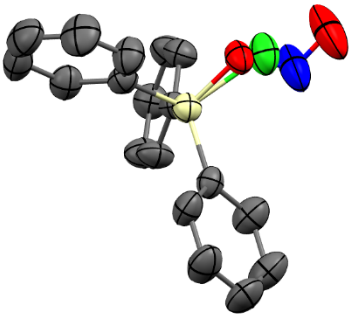

Figure S22: Asymmetric unit for the crystal structure of Ph_3SiONO, showing the substitutional disorder involving the Ph_3SiCl starting material. Hydrogen atoms were omitted for clarity. Selected bond distances (Å): Si-O 1.695(6), Si-Cl: 2.15(1), O-N 1.404(9), N=O 1.160(6). Selected bond angle (°): ONO 112.4(5).

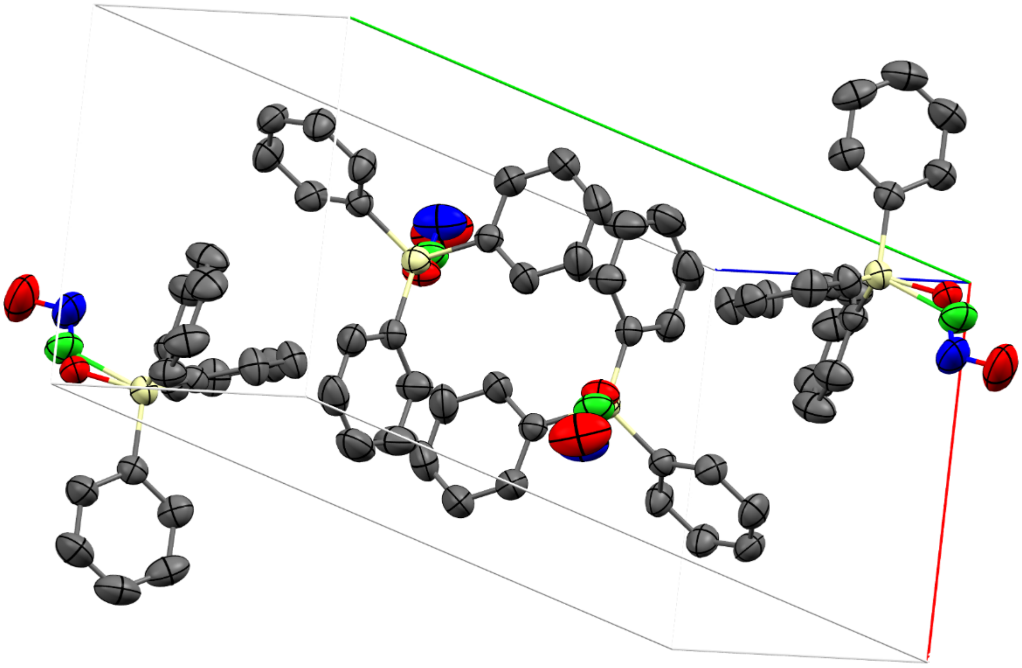

Figure S23: Unit cell of Ph_3SiONO, showing the substitutional disorder involving the Ph_3SiCl starting material. Hydrogen atoms were omitted for clarity.

Table S9: Experimental parameters for the structural determination of **6**.

Identification code	HD14-22_full2_refinz Ph_3SiONO (**6**)
Empirical formula	$C_{18}H_{15}N_{0.85}O_{1.7}SiCl_{0.15}$
Formula weight	303.80
Temperature/K	298.15
Crystal system	monoclinic
Space group	$P2_1/n$
a/Å	9.4177(7)
b/Å	18.4095(11)
c/Å	9.9867(7)
α/°	90
β/°	106.888(8)
γ/°	90
Volume/Å^3	1656.8(2)
Z	4
ρ_{calc}g/cm^3	1.218
μ/mm^{-1}	0.169
F(000)	636.0
Crystal size/mm^3	0.48 × 0.44 × 0.25
Radiation	Mo Kα (λ = 0.71073)
2Θ range for data collection/°	4.426 to 52.738
Index ranges	$-11 \leq h \leq 11$, $-23 \leq k \leq 22$, $-12 \leq l \leq 12$
Reflections collected	14783
Independent reflections	3357 [R_{int} = 0.0607, R_{sigma} = 0.0757]
Data/restraints/parameters	3357/0/209
Goodness-of-fit on F^2	0.987
Final R indexes [I>=2σ (I)]	R_1 = 0.0546, wR_2 = 0.1111
Final R indexes [all data]	R_1 = 0.1174, wR_2 = 0.1305

References

[1] M. J. Frisch, G. W. Trucks, H. B. Schlegel, G. E. Scuseria, M. A. Robb, J. R. Cheeseman, G. Scalmani, V. Barone,

G. A. Petersson, H. Nakatsuji, X. Li, M. Caricato, A. V. Marenich, J. Bloino, B. G. Janesko, R. Gomperts, B. Mennucci, H. P. Hratchian, J. V. Ortiz, A. F. Izmaylov, J. L. Sonnenberg, D. Williams-Young, F. Ding, F. Lipparini, F. Egidi, J. Goings, B. Peng, A. Petrone, T. Henderson, D. Ranasinghe, V. G. Zakrzewski, J. Gao, N. Rega, G. Zheng, W. Liang, M. Hada, M. Ehara, K. Toyota, R. Fukuda, J. Hasegawa, M. Ishida, T. Nakajima, Y. Honda, O. Kitao, H. Nakai, T. Vreven, K. Throssell, J. A. Montgomery, Jr., J. E. Peralta, F. Ogliaro, M. J. Bearpark, J. J. Heyd, E. N. Brothers, K. N. Kudin, V. N. Staroverov, T. A. Keith, R. Kobayashi, J. Normand, K. Raghavachari, A. P. Rendell, J. C. Burant, S. S. Iyengar, J. Tomasi, M. Cossi, J. M. Millam, M. Klene, C. Adamo, R. Cammi, J. W. Ochterski, R. L. Martin, K. Morokuma, O. Farkas, J. B. Foresman, and D. J. Fox, Gaussian, Inc., Wallingford CT, 2016.

[2] G. Sheldrick, Acta Crystallog*r. Sect. A: Found. Crystallogr. 2015, 71, 3-8.*

[3] G. *S*heldrick, Acta Crystallog*r. Sect. A: Found. Crystallogr. 2008, 64, 112-1***22.**

[4*]* O. V. Dolomanov, L. J. Bourhis, R. J. Gildea, J. A. K. Howard, H. Puschmann, J. Appl. Cryst. *2009, 42, 339-3***41.**